

Railway Subsidence Monitoring by High Resolution INSAR Time Series Analysis in Tianjin

Qingli Luo¹, Daniele Perissin^{1*}, Hui Lin¹, Qinghua Li¹, Ralf Duering²

¹ISEIS, Chinese University of Hong Kong, Hong Kong SAR, China

²Infoterra, Germany, Germany

* Corresponding author: daniele.perissin@cuhk.edu.hk

Abstract—Large-scale man-made linear features has played more and more important role in modern life and the development of urban are seriously affected by the subsidence of them. Permanent Scatterers (PS) technology was developed as a powerful tool for subsidence monitoring. High resolution of 1m data can be provided by TerraSAR X-band (TSX) with a short revisit period of 11days. More detail and sensitive subsidence information can be expected to be detected by X-band. In this paper, we exploited the potential of TSX for railway subsidence monitoring. A case study was conducted in Tianjin. A total of 37 TSX images acquired from 2009/4/29 to 2010/11/11 were used in PS analysis. The average deformation map and geocoded Permanent Scatterer were generated by SARPROZ

Keywords-TerraSAR; MST; railway; subsidence monitoring

I. INTRODUCTION

The rapid economic and urban city development in China takes much pressure on transportation. Large-scale man-made linear features, such as railway, highway and so on, have become the economic lifeline of each region. Railway subsidence monitoring has received extensive attention from all over the world. With excessive ground water withdrawal, Tianjin has become one of the major subsidence regions in China. Meantime, railway subsidence has become a serious problem, for not only the loss of financial investment but also lives at many places. Differential Interferometric Synthetic Aperture Radar (DINSAR) has been widely applied in subsidence monitoring for its all-time, all-weather and wide area monitoring ability, instead of traditional leveling and GPS. INSAR time series analysis technique was developed as a powerful tool for subsidence monitoring, avoiding time and space decorrelation and atmospheric disturbance. The published research on PS technology applications mainly aimed at monitoring region deformation, including urban land subsidence, mining land subsidence, volcanoes and earthquakes deformation, landslides and so on. Since large-scale man-made linear features has played more and more important role nowadays, much attention has been paid on the topic from scientists all over the world. Notwithstanding the great efforts made in researching the best approach, INSAR time series analysis is still far from being adopted as operative tools for railway subsidence monitoring.

The main drawback of SAR data till recent years has been the poor spatial resolution. With the launch of new generation high Resolution SAR satellites, the level of details visible in SAR

images increased dramatically [1, 2]. TerraSAR X-band (TSX) data provide 1m resolution. Moreover, the short revisit time of 11days as compared to the 35 day of ERS and ENVISAT favors a fast build-up of interferometric data stacks [3]. The very high resolution TSX data should be used wisely for identifying targets that need detailed information [4, 5].

In this paper, we introduce the research carried out at the Institute of Space and Information Science of Hong Kong on railway time series analysis subject. The output of the work will be useful to drive future policies of railway subsidence monitoring. The main aim of our work was to exploit the potential of TSX data for railway subsidence monitoring and more detail information are expected to be detected by X-band data. A case study was conducted in Tianjin, one of the major subsidence cities in China.

II. STUDY AREA AND TSX DATA

The case study area is located in the west of Tianjin downtown. Subsidence is one of the most important geological disasters in Tianjin. Since 1959, the max accumulated subsidence has achieved to 2.95m, the average subsidence rate from 1985 to 2005 reaches up to 29.99mm [6] and the subsidence area is almost 8000km [7]. Subsidence seriously affects construction and maintain of infrastructures so that it prevent urban from rapid development [7]. Moreover, Jingjin highspeed railway was built along 117 km between Beijing and Tianjin and the maximum speed reaches to 350km/h. With high speed and frequency schedule of the railway, slight subsidence could bring more risks for the life of passengers.



Figure 1. Location of TerraSAR-X data from google earth

We applied PS technology to monitor the railway subsidence in Tianjin. Figure 1 shows the location of the TSX data. The exploited SAR data set was constructed from 37 TSX stripmap images acquired from 2009/4/29 to 2010/11/11. The incidence angle is 41° . The center latitude and longitude is 39.20° , 116.91° , respectively. TSX data are provided by Infoterra, Germany. Table 1 reports the acquisition data and baseline of the related images. The image coverage area is 30^*50km^2 with the pixel spacings of 1.36 m in slant and 1.90m in Azimuth. As SLC reference geometry, we used the scene acquired on Nov, 13th, 2009.

Table 1. TSX data and description

Scenes	Date (yy/mm/dd)	Baseline (m)	Interval (days)	Height ambiguity
1	20090429	13	-198	522
2	20090510	30	-187	226
3	20090521	64	-176	106
4	20090601	42	-165	161
5	20090623	-76	-143	-89
6	20090704	-17	-132	-399
7	20090715	-33	-121	-206
8	20090726	-112	-110	-61
9	20090806	137	-99	50
10	20090828	-101	-77	-67
11	20090908	36	-66	188
12	20090919	-64	-55	-106
13	20090930	-181	-44	-37
14	20091011	-39	-33	-174
15	20091022	-65	-22	-104
16	20091102	119	-11	57
17	20091113	0	0	-
18	20091124	46	11	147
19	20091205	126	22	54
20	20091216	122	33	56
21	20091227	133	44	51
22	20100107	-24	55	-283
23	20100118	-26	66	-261
24	20100129	-7	77	-969
25	20100220	-154	99	-44
26	20100303	-151	110	-45
27	20100314	-104	121	-65
28	20100325	10	132	678
29	20100405	-93	143	-73
30	20100416	-126	154	-54
31	20100427	-37	165	-183
32	20100621	18	220	377
33	20100702	-78	231	-87
34	20100804	81	264	84
35	20100906	1	297	6782
36	20101009	159	330	43
37	20101111	-23	363	-295

III. PS ANALYSIS

PS technology has been approved as an effective tool for wide area subsidence monitoring within mm level accuracy and meters of spatial resolution. TSX, launched on June 15th, 2007, is a German high resolution radar satellite. Most of the current INSAR processing algorithms can be applied into TSX data without fundamental modifications. In order to achieve optimal interferometric results, the key processing steps are emphasized in this study. The processed area is about 10 sqkm wide and the reflectivity map is shown as Figure 2.

A. Interferogram generation

After SLC coregistration, we can then generate interferograms from multi-temporal SAR images. There are three different choices to construct interferometric pairs, including classical star image graph, small baseline, Minimum Spanning Tree (MST). In the traditional PSI technology, one master image is selected and the image graph looks like star. [8]. Small baseline was proposed [9, 10] to reduce the geometric or temporal. For fully considering both temporal and spatial decorrelation, MST interferogram generation method was developed [11], creating a different framework for optimal interferometric pairs selection. The core idea is to search the minimum best coherence graph connecting all the images from the multi SAR images, without using any predefined decorrelation model (temporal or spatial), simply by maximizing the interferometric coherence[8]. Since small baseline has the drawback that some of the available images may not be used and the image graph is often disconnected and that will prevent the correct motion measurement, we just compare the traditional one master acquisition and MST image graph of TSX data in this area as Figure 3.

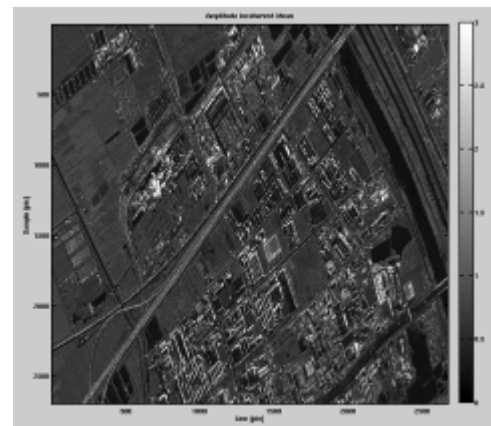


Figure 2. The reflectivity map

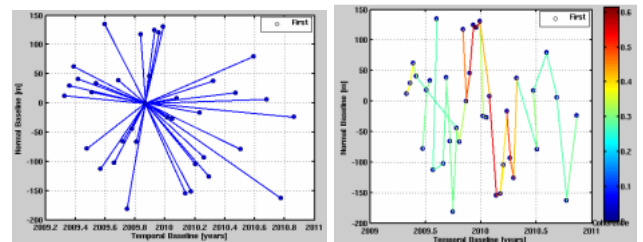


Figure 3. Left: Traditional image graph; Right: MST image graph

The two image graphs of Figure 3 show the X band dataset with temporal and spatial baseline. In particular, MST image graph shows the average coherence of each interferogram and the color bar gives the value from 0 to 0.6 as Figure 3 Right. In fact, most connections of MST graph are mainly vertical and this means small temporal baselines are selected. When time interval is long, the problem of phase decorrelation is significant. One of the possible reasons should be the ground affected by strong motion. Meanwhile, another possible explanation is related to the management of fields in the Tianjin area: it is in fact common in this region to cover cultivated plants with a structure for protecting them from bad weather

conditions. This kind of changes of the ground surface makes it complex to interpret the spatial coherence and causes the failure of common models of the spatio/temporal behavior of the InSAR phase. Moreover, from Figure 3 we can notice, as a general comment, that we have a set of coherent images between the end of 2009 and the beginning of 2010 (yellow-red color), while much worse performances are registered at the beginning and at the end of our dataset (light blue color). We also observe that from spring 2010 we have less data separated by longer temporal baselines, making it more difficult to precisely estimate and reconstruct motion time series of PSs. Starting from the above considerations, we decided to process the area of interest with a common PS approach, using a star graph with a common master image as Figure 3 Left.

B. PS candidate identification

For PS candidate identification, there are two classical methods: spectral diversity and amplitude dispersion index. Spectral diversity selected a dominant pointlike scatterer. Since pointlike scatterers are not affected much by geometric decorrelation, they are suited well even if long baseline interferograms are included. For amplitude dispersion index, the pixel whose backscattering is not changed so much with time will be selected as PS candidate. We applied amplitude dispersion index to select PS candidate and apply it for PSI analysis. Although the interval of the TSX images is short, the distribution of the candidates is also inhomogeneous. There are more PS points in urban areas and less in rural area within the same size as the Figure 4 shows.

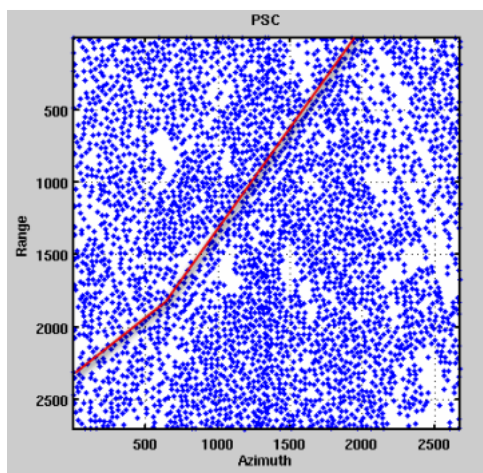


Figure 4. The PSC (the red line means the railway)

C. Average deformation map and displacement history

For phase unwrapping of PS analysis, the deformation velocity and height correction between neighboring PS candidates can be estimated by applying 2-D periodogram in time domain. After removing the Atmospheric Phase Screen (APS), we can estimate the average deformation velocity and retrieve the deformation history of a selected PS. Then, the location of railway can be identified and finally, we can get the result of railway subsidence.

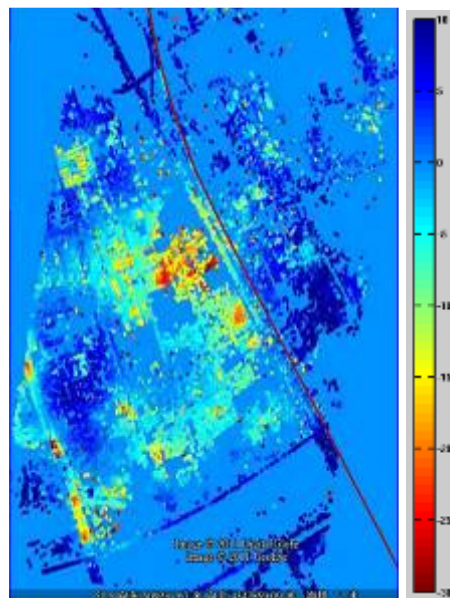


Figure 5. Linear deformation trend in the selected area, resampled on a regular grid in geographical coordinates. The red line crossing the image represents the path of the Jingjin Highspeed Railway. The color scale shows rates between -30 and 10 mm/year to a reference point assumed stable. It is interesting to notice that the path of the railway (depicted in Figure 12) could be affected by a considerable deformation at the center of the image. Another important phenomenon to observe is several much localized subsidences on a highway at the lower left corner of the image.

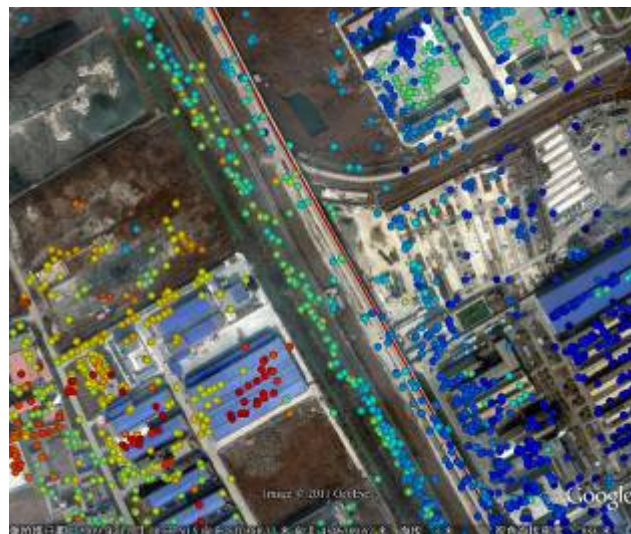


Figure 6 The geocoded Permanent Scatterer in Google earth

Figure 6 shows a close up on a set of PSs geocoded in Google Earth, with the same color scale as Figure 5. The area is crossed by the railway. At the left side of the railway, stronger subsidence is detected, affecting also the path of the train. One selected PS is shown in Figure 7 and the corresponding displacement time history (referred to a target belonging to the same area) is shown in Figure 8. As clearly visible, the deformation trend is complex and not simply linear. In fact, the

entity of the estimated motion in this area is around 30 mm/year.

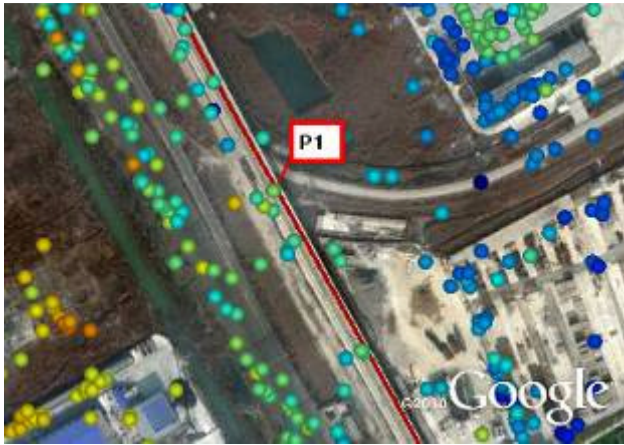


Figure 7. The selected PS named P1.

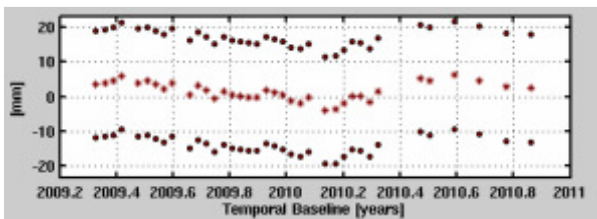


Figure 8. Example of displacement history of P1.

IV. CONCLUSION AND PERSPECTIVES

Figure 4 shows the detail of the railway distribution and also give us the hint that TSX can provide high PS candidate density and it is possible for us to exploit TSX data for railway subsidence monitoring. Meanwhile, we can acquire another good conclusion from Figure 5. Although X-band is more easily affected by temporal decorrelation, the railway, one of the most important large-scale linear man-made infrastructures, can be monitored in detail by TSX data. For relatively long time interval, the man-made infrastructures maintain relatively good coherence. The average deformation map and geocoded PS were generated and the results show that X-band owns the strong potential for railway subsidence monitoring.

There are still some drawbacks for railway subsidence by only applying high resolution SAR. The wavelength of TSX data is 3.1cm, relatively short and the subsidence rate that can be detected is within 50cm per year. Then, combining other SAR data could provide more reliable subsidence monitoring results. For rural area, since the vegetation is changing within time, the

temporal coherence is decreased with time for X-band and it is not easy to acquire reliable subsidence monitoring results in this area. Railway is constructed bestriding both urban and rural area. Thus, solutions for rural area are necessary for monitoring railway subsidence.

ACKNOWLEDGMENT

TerraSAR-X data used in this work are provided by Infoterra. The software we used in this work is SARProz, developed by Daniele Perissin. The authors are very thankful to the support of the Research Grants Council of HKSAR (Ref. No.450210) and the project name is an integrated model for monitoring Qinghai-Tibet railway deformation based on DInSAR technology and GPS observations.

REFERENCES

- [1] Inglada, J. and G. Mercier, "A new statistical similarity measure for change detection in multitemporal SAR images and its extension to multiscale change analysis", *Geoscience and Remote Sensing, IEEE Transactions on*, 2007. 45(5): p. 1432-1445.
- [2] Sabry, R., "A New Coherency Formalism for Change Detection and Phenomenology in SAR Imagery: A Field Approach", *Geoscience and Remote Sensing Letters, IEEE*, 2009. 6(3): p. 458-462.
- [3] Adam, N., X. Zhu, and R. Bamler, "Coherent stacking with TerraSAR-X imagery in urban areas", in *Urban Remote Sensing Event, 2009 Joint* 2009.
- [4] Baade, J. and C.C. Schullius, "Interferometric Microrelief Sensing With TerraSAR-X-First Results", *IEEE Transactions on Geoscience and Remote Sensing*, 2010. 48(2): p. 965-970.
- [5] Hong, S.H., S. Wdowinski, and S.W. Kim, "Evaluation of TerraSAR-X Observations for Wetland InSAR Application", *IEEE Transactions on Geoscience and Remote Sensing*, 2010. 48(2): p. 864-873.
- [6] Hu, B., et al., "Assessment and Zonation of Land Subsidence Disaster Risk in Urban and Suburb of Tianjin", *CHINA POPULATION, RESOURCES AND ENVIRONMENT*, 2008. 18(4): p. 28-34.
- [7] YU, Q., W. W., and C. YI, "Design and Application of an Automatic System for Land-subside and Water Table Monitoring in Tianjin City", *Ground Water*, 2007. 5.
- [8] Prati, C., A. Ferretti, and D. Perissin, "Recent advances on surface ground deformation measurement by means of repeated space-borne SAR observations", *Journal of Geodynamics*, 2009. 49(3-4): p. 161-170.
- [9] Lanari, R., et al., "A small-baseline approach for investigating deformations on full-resolution differential SAR interferograms", *Geoscience and Remote Sensing, IEEE Transactions on*, 2004. 42(7): p. 1377-1386.
- [10] Berardino, P., et al., "A new algorithm for surface deformation monitoring based on small baseline differential SAR interferograms", *Geoscience and Remote Sensing, IEEE Transactions on*, 2002. 40(11): p. 2375-2383.
- [11] Perissin, D., et al., "LANDSLIDE IN DOSSENA (BG): COMPARISON BETWEEN INTERFEROMETRIC TECHNIQUES", *BIOGEOSAR*, 2007. 9.